

Critical hybridization for the Kondo resonance in gapless systems

R. G. Dias, Lidia del Rio, and A. V. Goltsev
Departamento de Fısica, Universidade de Aveiro,
3810 Aveiro, Portugal
 (Dated: February 13, 2022)

We study the Kondo resonance in a spin-1/2 single impurity Anderson model with a gapless conduction band using the equation of motion approach in order to obtain the impurity spectral function. We study two different scenarios for gapless systems: a purely power-law energy dependence of the density of states or a constant density of states with a gapless behavior near the Fermi level. We demonstrate that strong electron-electron correlations lead to a sharp peak in the impurity spectral function in the case of a large exchange coupling ($J > J_c$) or equivalently, a strong hybridization ($V > V_c$). This Kondo-like peak emerges much below the Fermi level in the case of a strongly depleted density of states. These results are compared with the ones from renormalization group approaches.

PACS numbers:

I. INTRODUCTION

The advent of graphene has renewed the interest in the Kondo effect in gapless systems.[1] It is known that a strong depletion of the density of states of a conduction band near the Fermi level modifies the usual behavior of magnetic and nonmagnetic impurities.[2, 3] Impurities in gapless systems have been addressed, for instance, in the context of d-wave superconductors [4, 5, 6] and more recently graphene,[7] using a variety of methods, from renormalization group approaches [8, 9, 10, 11] to the large N analysis [12] and T-matrix calculations.[13] The most relevant modification in gapless systems of the usual Kondo behavior is the requirement of a finite critical Kondo coupling strength in order to observe the Kondo resonance.[2, 7] While several renormalization group studies have addressed this point [2, 3, 7], an equivalent study from the point of view of the impurity spectral function in the case of the single impurity Anderson model has not been carried out as far as we know. In the present manuscript, we address this problem using the equation of motion (EOM) approach which has been successful in describing the Kondo resonance in systems with a finite density of states at the Fermi level.[14] The nonmagnetic case when the on-site Coulomb repulsion is zero ($U = 0$), and the strong on-site Coulomb repulsion limit ($U \rightarrow \infty$) of the gapless single impurity Anderson model are considered. Note that above the Kondo temperature, the $U \rightarrow \infty$ spectral function should recover the $U = 0$ features. We will show that even for $U = 0$, an additional peak may appear in the spectral function due to the depletion of the density of states which should not be confused with a Kondo peak. We will demonstrate that the critical exchange coupling depends strongly on the density of states profile in the gapless region. Furthermore, the strong electron-electron correlations can produce a strong Kondo-like peak in the impurity spectral function even much below the Fermi level in the depletion region. This Kondo-like peak emerges if the hybridization between the conduction band and the impurity is

larger than a critical value, which in turn is determined by the energy dependence of the density of states in the depletion region, and grows with decreasing temperature.

II. GAPLESS ANDERSON HAMILTONIAN

The single impurity Anderson model is given by

$$H = \sum_{k\sigma} \varepsilon_k \hat{n}_{k\sigma} + \sum_{\sigma} E_0 \hat{n}_{d\sigma} + \frac{1}{2} U \sum_{\sigma} \hat{n}_{d\sigma} \hat{n}_{d\bar{\sigma}} + V \sum_{k\sigma} (c_{k\sigma}^{\dagger} d_{\sigma} + d_{\sigma}^{\dagger} c_{k\sigma}). \quad (1)$$

where the standard notations[15] are used: V is the hybridization between conduction and impurity states, and E_0 is the impurity energy level. In order to describe gapless systems, a density of states with a power-law energy dependence is usually considered in a certain energy interval around the Fermi energy which we set at $\varepsilon_F = 0$. We will assume that the density of states of the conduction band is constant outside this interval, $\rho(\varepsilon) = \rho_0$, for $D_1 < |\varepsilon| < D$, and $\rho(\varepsilon) = \rho_1(\varepsilon) = \alpha|\varepsilon|^{\gamma}$ for $|\varepsilon| < D_1$ with $\alpha = \rho_0/D_1^{\gamma}$. Therefore, $\rho(\varepsilon)$ is zero at the Fermi level. The bandwidth is $2D$. In Fig. 1, the density of states for several values of γ is shown. In graphene, $\gamma = 1$. If $D_1 = 0$, then one has a constant density of states with the finite bandwidth. If $D_1 = D$, only the power-law dependence of the density of states is considered. $\gamma = \infty$ corresponds to a system with a $2D_1$ gap. Below, we will discuss in detail the case $E_0 < -D_1$.

III. EQUATION OF MOTION METHOD

The equation of motion approach is basically the successive application of the result $\omega G_{AB}(\omega) = \langle \{A, B\} \rangle + \langle \langle [A, H]; B \rangle \rangle_{\omega}$ to the impurity Green's function and to the other Green's function generated in the process.[14]

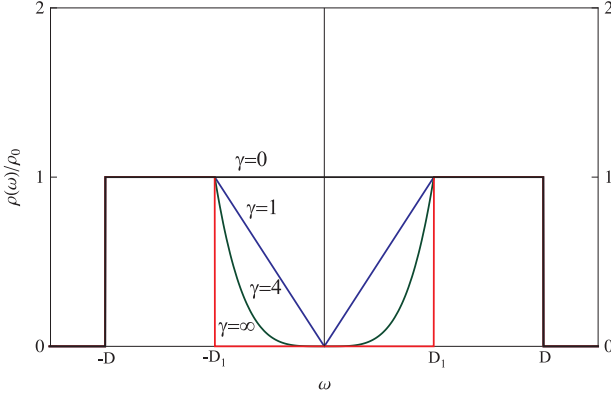


FIG. 1: The density of states $\rho(\omega)$ of the conduction band used in this article. The density of states is constant in the energy range $D_1 < |\omega| < D$ and has a power-law dependence $\rho(\omega) = \alpha|\omega|^\gamma$ for $|\omega| < D_1$. The density of states profile for several γ values is displayed. Note that $\gamma = \infty$ implies the existence of a $2D_1$ energy gap.

Here we have adopted the Zubarev notation for the retarded Green's function, $G_{A,B}(\omega) = \langle\langle A; B \rangle\rangle_\omega$. [16] As usual, it is implicit that $\omega \rightarrow \omega + i\eta$ where η is a infinitesimal positive constant. In the case of the Anderson model, one obtains the following EOM for the impurity Green's function

$$\left(\omega - E_0 - \sum_k \frac{V^2}{\omega - \varepsilon_k} \right) \langle\langle d_\sigma; d_\sigma^+ \rangle\rangle_\omega = 1 + U \langle\langle \hat{n}_{d\bar{\sigma}} d_\sigma; d_\sigma^+ \rangle\rangle_\omega. \quad (2)$$

If the on-site repulsion between electrons is neglected ($U = 0$), this equation becomes a closed EOM. Below, we discuss this $U = 0$ case in detail before addressing the $U \rightarrow \infty$ limit for two reasons. First, due to the depletion of the density of states at the Fermi level, the $U = 0$ impurity spectral function will have a non trivial dependence on the impurity energy level and on the hybridization value V . In particular, it may display more structure than the typical Lorentzian profile. This more complex profile is the background against which the correlation effects will be observed in the $U \rightarrow \infty$ limit. Second, the $U = 0$ features should be recovered in the $U \rightarrow \infty$ spectral function above the Kondo temperature.

IV. RESONANT LEVEL ($U = 0$)

The self-energy for $U = 0$ can be easily obtained for integer γ and is given by

$$\Sigma_0 = \sum_k \frac{V^2}{\omega - \varepsilon_k} = \Lambda(\omega) - i\Delta(\omega), \quad (3)$$

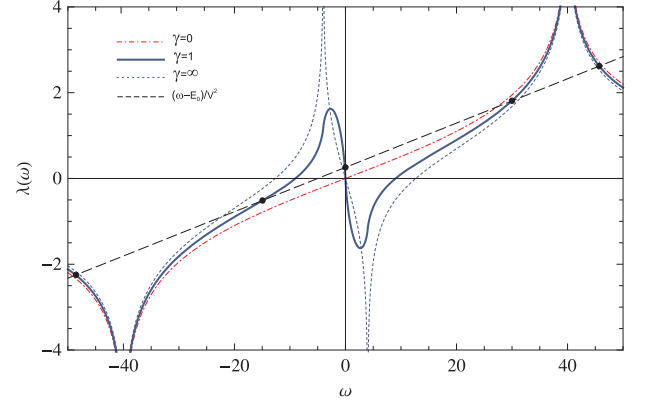


FIG. 2: The real part $\lambda(\omega)$ of the self-energy Σ_0 , Eq. (5), for the resonant level ($U = 0$) exhibits logarithmic divergences at the band edges and a non-monotonous behavior in the gapless frequency region. The dashed line represents the line $(\omega - E_0)/V^2$. The black points are the roots of $\omega - E_0 - \Lambda(\omega)$. For $\gamma = \infty$ (the gapped spectrum), additional logarithmic divergences are present at the gapless region edges. Parameters: $E_0 = -5$, $\rho_0 = 1$, $V = 4.4$, $D_1 = 4$ and $D = 40$.

with

$$\frac{\Delta(\omega)}{V^2} = \tau(\omega) = \pi\rho(\omega) + \eta, \quad (4)$$

$$\frac{\Lambda(\omega)}{V^2} = \lambda(\omega) = B(\omega) + P_n(\omega) + \rho_0 \ln \left| \frac{(D + \omega)(D_1 - \omega)}{(D - \omega)(D_1 + \omega)} \right|, \quad (5)$$

where

$$B(\omega) = \begin{cases} \alpha\omega^\gamma \ln \left| \frac{\omega^2}{D_1^2 - \omega^2} \right|, & \gamma \text{ odd}, \\ \alpha\omega^\gamma \ln \left| \frac{D_1 + \omega}{D_1 - \omega} \right|, & \gamma \text{ even}, \end{cases} \quad (6)$$

and $P_n(\omega)$ is a polynomial of degree $n < \gamma$. For $\gamma = 1$ and $\gamma = \infty$ (a gapped conduction band), $P_n(\omega) = 0$. In Fig. 2, the real part of the self-energy Σ_0 is displayed for $\gamma = 0$, $\gamma = 1$ and $\gamma = \infty$ (the gapped spectrum).

The spectral function $\mathcal{A}(\omega) = -2 \text{Im} \langle\langle d_\sigma; d_\sigma^+ \rangle\rangle_\omega$ for a system with finite bandwidth (gapless or not) is given by

$$\mathcal{A}(\omega) = \frac{2\Delta(\omega)}{[\omega - E_0 - \Lambda(\omega)]^2 + \Delta^2(\omega)} + 2\pi\Theta(D - |\omega|) \sum_i |1 - \Lambda'(\omega)|^{-1} \delta(\omega - \omega_i) \quad (7)$$

where ω_i are the roots of $\omega - E_0 - \Lambda(\omega) = 0$. Note that the Dirac delta points outside the band continuum play an important role if the hybridization is not small. These points are essential in order to satisfy the sum rule of the spectral function. This can be more clearly understood

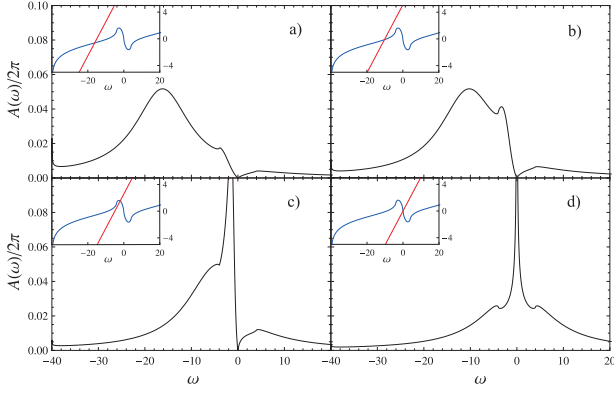


FIG. 3: The spectral function $A(\omega)$, from Eq. (7), for the resonant level ($U = 0$) for $\gamma = 1$ and several values of the impurity level energy: a) $E_0 = -15$; b) $E_0 = -10$; c) $E_0 = -5$; d) $E_0 = 0$. Inset: The real part of the self-energy $\lambda(\omega)$ and the line $(\omega - E_0)/V^2$. It is the non-monotonous behavior of $\lambda(\omega)$ that generates additional structure in the spectral function for certain intervals of the parameters. For small V , this structure disappears. Other parameters: $\rho_0^{1/2}V = 1.4$, $D_1 = 4$ and $D = 40$.

if the continuous term is written as

$$\frac{1}{V^2} \frac{2\gamma(\omega)}{\left[\frac{\omega}{V^2} - \frac{E_0}{V^2} - \lambda(\omega) \right]^2 + \tau^2(\omega)}. \quad (8)$$

Therefore, for large V and a constant density of states most of the spectral weight is associated with the Dirac delta points outside the band continuum since the total spectral weight for $|\omega| < D$ decays as $1/V^2$. As can be inferred from Fig. 2, for large V [or equivalently a small slope of the straight line $(\omega - E_0)/V^2$], the Dirac delta points are located at large ω . For large ω , $\Lambda(\omega) \sim V^2 C/\omega$ where $C \sim \rho_0 D$ and therefore $\omega_i = \pm V\sqrt{C}$ leading to $|1 - \Lambda'(\omega)|^{-1} \sim 1/2$. Thus the sum rule is satisfied. For small V , these Dirac delta points are located near the boundaries of the band due to the log-like behavior of $\Lambda(\omega)$. The same conclusion holds for a power-law density of states.

For a constant density of states, $\lambda(\omega)$ is monotonous for $|\omega| < D$ and the minima of the first term in the denominator of the spectral function given by Eq. (8) are typically roots of $\omega - E_0 - \Lambda(\omega)$. In the case of a power-law density of states, additional minima appear due to the non-monotonous behavior of $\Lambda(\omega)$ within the gapless region. These minima are not necessarily roots of $\omega - E_0 - \Lambda(\omega)$, but lead to an additional structure in the spectral function. In Fig. 3, the spectral function for $U = 0$ at several values of E_0 is displayed. For general γ , one has a $|\omega|^\gamma$ behavior of the spectral function near the Fermi energy, except for $E_0 = 0$ as can be observed in Fig. 3. It is worthwhile to emphasize that the impurity spectral function exhibits the same depletion at the Fermi level as the density of states of the conduction band.

Note that the value of V determines the slope of the

line $(\omega - E_0)/V^2$ leading to different behavior of the spectral function. A small V implies a large slope and typically only one root of $\omega - E_0 - \Lambda(\omega)$ for $|\omega| < D$. For large V , one has an almost horizontal line intersecting the $\lambda(\omega)$ curve in Fig. 2. The same reasoning applies in the interacting case that will be considered below. Since the V^2 terms appear always associated to a ρ_0 factor in the spectral function, these parameters play equivalent roles.

It is important to emphasize that a root of $[\omega - E - \Lambda(\omega)]$ is not a maximum of the spectral function if this root is within the gapless region of the density of states. In fact, given a function $g(x) = x/[f^2(x) + x^2]$ where $f(x)$ is a function with a local peak at $x = x_0$, then the corresponding peak in $g(x)$ will be at $x'_0 = x_0\{1 + 1/[f'(x_0)]^2\}^{-1/2}$ and therefore $x \approx x_0$ if $f' \gg 1$ or $x \approx 0$ if $f' \ll 1$. Furthermore, if the root is near the Fermi level, the respective peak in the spectral function becomes very narrow, but the total spectral weight associated with the peak becomes very low. This can be easily concluded since the spectral function [Eq. (8)] for $\gamma = 1$ can be written in the neighborhood of the roots ω_i (if $|\omega_i| < D_1$) as $c|\omega|\mathcal{F}(\omega)$, where $\mathcal{F}(\omega)$ is a normalized Lorentzian with center at $\omega_i/[1 + \kappa^2]$ and half-width $|\kappa/(1 + \kappa^2)| \cdot \omega_i$, where $\kappa = \pi\alpha V^2/|1 - \Lambda'(\omega_i)|$ and $c = \pi|1 - \Lambda'(\omega_i)|^{-1}|\kappa/(1 + \kappa^2)|$. For small $|\omega_i|$, $\Lambda'(\omega_i)$ becomes large and κ becomes small, and therefore one has a narrow peak with a low spectral weight. The linear factor leads to a shift of the maximum of the Lorentzian away from zero frequency to $\omega_i/[1 + \kappa^2]^{1/2}$.

V. THE KONDO RESONANCE ($U = \infty$)

In the $U \neq 0$ case, the equation of motion for the last term in Eq. (2) has to be considered. Adopting the Appelbaum and Penn approximation,[17] one finds the following expression for the impurity Green's function for $U = \infty$,

$$(\omega - E_0 - \Sigma_0 - \Sigma_1 - \Sigma_2) \langle \langle d_\sigma; d_\sigma^\dagger \rangle \rangle_\omega = 1 - \langle n_{d\bar{\sigma}} \rangle - V \sum_k \frac{\langle d_\sigma^\dagger c_{k\bar{\sigma}} \rangle}{\omega - \varepsilon_k}, \quad (9)$$

where

$$\Sigma_1 = V^2 \sum_{k,k'} \frac{\langle c_{k'\bar{\sigma}}^\dagger c_{k\bar{\sigma}} \rangle}{\omega - \varepsilon_k}, \quad (10)$$

$$\Sigma_2 = V^3 \sum_{k,k'} \frac{\langle d_\sigma^\dagger c_{k\bar{\sigma}} \rangle}{(\omega - \varepsilon_k)(\omega - \varepsilon_{k'})}, \quad (11)$$

and Σ_0 is given by Eq. (3). In order to describe qualitatively the Kondo resonance, one has to understand the temperature behavior of the low order self-energy Σ_1 . For sufficiently small V , one can neglect Σ_2 and the Kondo resonance will be generated by Σ_1 , which is

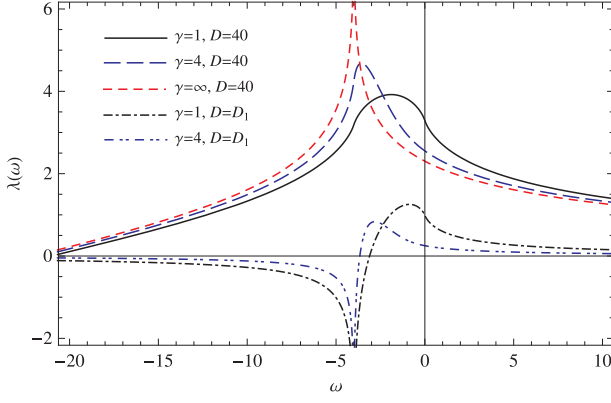


FIG. 4: The real part of the zero temperature self-energy $\lambda_1(\omega) = \text{Re}[\Sigma_1(\omega, 0)]/V^2$ for several values of γ . In the case of $\gamma = \infty$, there is a gap, $N(\epsilon) = 0$ at $|\omega| < D_1$, which leads to a logarithmic divergence of the real part of the self-energy at the gap edge. Other parameters: $\rho_0 = 1$, $D_1 = 4$, and $D = 40$ or $D = D_1$.

approximately given by

$$\frac{\Sigma_1(\omega, T)}{V^2} \approx -i\pi\rho(\omega)f(\omega) + \int d\omega' \rho(\omega')f(\omega')P\left(\frac{1}{\omega - \omega'}\right). \quad (12)$$

The Fermi-Dirac distribution function $f(x)$ sets a high energy cutoff in the previous integral which, for $\gamma = 1$, is approximately given by

$$\text{Re}\left[\frac{\Sigma_1(\omega, T)}{V^2}\right] \approx \rho_0 \ln\left|\frac{D + \omega}{D_1 + \omega}\right| + \alpha(D_1 - k_B T) + \alpha\omega \ln \frac{\sqrt{\omega^2 + (ak_B T)^2}}{|D_1 + \omega|}, \quad (13)$$

for $k_B T < D_1$ and $a \sim \pi$. We would like to note that in our numerical solution of Eq. (9), the self-energy Σ_2 is taken into account.

The previous expression should be compared with the Lacroix result for a constant density of states,[14]

$$\text{Re}\left[\frac{\Sigma_1(\omega, T)}{V^2}\right] \sim -\rho_0 \ln \frac{\sqrt{\omega^2 + (\pi k_B T)^2}}{D}. \quad (14)$$

The most relevant difference between the previous two expressions is the temperature behavior. For a constant density of states, $\text{Re}(\Sigma_1)$ diverges at zero temperature as $\omega \rightarrow 0$. For the gapless density of states, as the temperature goes to zero, $\text{Re}(\Sigma_1)$ remains finite at the Fermi energy (as shown in Fig. 4) with a peak in the energy range $-D_1 < \omega < 0$. Note that for a strong depletion of the density of states this peak grows and approaches the gapless region edge, converging therefore to the logarithmic divergence of the real part of the self-energy of an equivalent system with a $2D_1$ gap. In Fig. 4, the self-energy for a linear and the quartic density of states with

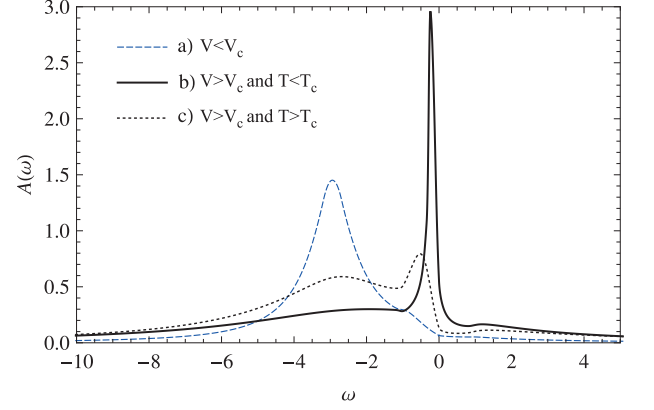


FIG. 5: The spectral function $A(\omega)$, for $U = \infty$, $\gamma = 1$, and several values of the hybridization V . Curve a) displays the typical $V < V_c$ spectral function characterized by the absence of a Kondo resonance. The Kondo peak appears as V is increased above a critical value V_c [curve b)] and disappears above the Kondo temperature T_c [curve c)]. Other parameters: $E_0 = -3.2$, $\rho_0 = 10$, $D_1 = 1$, $D = 20$ and a) $V = 0.12$, $k_B T = 0.05$; b) $V = 0.24$, $k_B T = 0.05$; c) $V = 0.24$, $k_B T = 10$.

$D = D_1$ is also displayed. The self-energy of the latter is strongly reduced in the $-D_1 < \omega < 0$ region due to the absence of the log-like contribution which resulted from the $-D < \omega < -D_1$ constant term in the density of states.

A. The critical hybridization

The critical temperature for the Kondo resonance in the equation of motion approach [14] is associated with a temperature below which a new solution of $\text{Re}[\langle d_\sigma; d_\sigma^\dagger \rangle_\omega^{-1}] = 0$ appears. This solution is due to an additional intersection between the line $\omega - E_0$ and the real part of the self-energy $\text{Re}(\Sigma_1)$. In the case of a constant density of states, this solution occurs near $\omega = 0$. Since the maximum value of the self-energy for the constant density of states ($\gamma = 0$) is

$$\text{Re}\left[\frac{\Sigma_1(0, T)}{V^2}\right] \sim -\rho_0 \ln\left(\frac{\pi k_B T}{D}\right) \quad (15)$$

and decreases with increasing temperature, above a critical temperature one loses the additional intersection and the Kondo peak disappears. The condition $E_0/V^2 \sim \rho_0 \ln(k_B T_c/D)$ determines the Kondo temperature. Note that this condition has a solution for any value of V , however small it may be, due to the logarithmic dependence on temperature.

In the case of the gapless density of states (with $\gamma \geq 1$), the same reasoning can be followed in order to obtain the critical temperature. However, the real part of the self-energy Σ_1 does not diverge at zero temperature for any frequency (excluding the band edges). Therefore, for

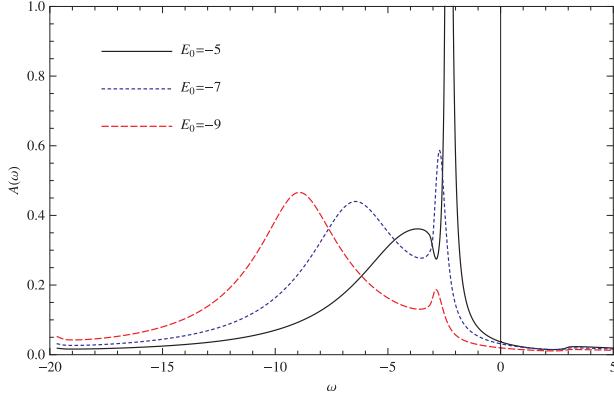


FIG. 6: The spectral function $A(\omega)$ for $U = \infty$, $\gamma = 8$, and several values of the impurity energy, $E_0 = -5, -7$ and -9 . One can see that when E_0 increases and approaches the edge of the depletion region ($\omega = -3$, on this figure), the Kondo peak grows within the depletion region much below the Fermi energy. Other parameters: $\rho_0 = 10$, $D_1 = 3$, $D = 20$, $V = 0.2$, and $k_B T = 0.05$.

a sufficiently small hybridization, the Kondo peak does not occur. In the case of $\rho(\omega) = \alpha|\omega|^\gamma \Theta(D_1 - |\omega|)$, the real part of the self-energy for large γ can be obtained expanding the density of states at $\omega = -D_1$ and is given approximately by

$$\text{Re} \left[\frac{\Sigma_1(\omega, 0)}{V^2} \right] \approx \alpha D_1^\gamma + \alpha D_1^\gamma \left[1 - \gamma \left(1 + \frac{\omega}{D_1} \right) \right] \times \ln \left| 1 - \frac{1/\gamma}{1 + \frac{\omega}{D_1}} \right| \quad (16)$$

This function has a maximum at ω_{max} given by $\omega_{max} + D_1 \sim 3D_1/4\gamma$ and approximately of the value of ρ_0 . The constant behavior of the density of states in the energy interval $-D < \omega < -D_1$ leads to an additional $\rho_0 V^2 \ln |(D + \omega)/(D_1 + \omega)|$ term in the real part of the self-energy, $\text{Re}[\Sigma_1(\omega, 0)]$. For $D \gg D_1$, the maximum of the real part of the self-energy is shifted to $\omega_{max} + D_1 \sim D_1/2\gamma$ and its value is approximately $\rho_0 V^2 \ln(2\gamma D/D_1)$ which is the same as the former maximum value except for an enhancement factor $\ln(2\gamma D/D_1)$. Note that this enhancement reflects the contribution of the constant density of states region. In fact, for large γ , the behavior becomes similar to a gapped system. In Fig. 4, the difference between the maximum values of $\text{Re}[\Sigma_1(\omega, 0)]$ for $D \gg D_1$ and $D = D_1$ is clearly observed as well as the shift of the maximum position (with increasing γ) towards the negative edge of the gapless region.

The critical hybridization is the minimum V which is necessary to have an intersection between the line $\omega - E_0$ and $\text{Re}[\Sigma_1(\omega, 0)]$ at zero temperature. For $E_0 \lesssim -D_1$, one has to take into account that the maximum occurs at ω_{max} and the condition for the critical hybridization becomes for $\gamma \gtrsim 1$

$$\frac{\omega_{max} - E_0}{V^2} \approx \begin{cases} \alpha D_1^\gamma \ln(2\gamma D/D_1), & D \gg D_1, \\ \alpha D_1^\gamma, & D = D_1. \end{cases} \quad (17)$$

It is necessary to note that the density of states used in the renormalization group approach [2] corresponds to $D = D_1$. For not so large γ , this density of states is reasonable, but in the $\gamma \rightarrow \infty$ limit, this density of states becomes unrealistic since the electron states are concentrated in a narrow region at the band edges. Equation (17) should be compared with the expression for the critical exchange coupling J_c of the spin-1/2 Kondo model with a gapless conduction band, $J_c \approx \gamma/\alpha D_1^\gamma = \gamma/\rho_0$. [2] The Kondo model can be obtained from the Anderson model within perturbation theory [15] leading to an exchange coupling $J_{\mathbf{k}\mathbf{k}'} \sim V^2/(\varepsilon_{\mathbf{k}} - E_0)$ which is antiferromagnetic for energies $\varepsilon_{\mathbf{k}} \sim 0$. The resonant scattering of the conduction electrons in that energy region leads to the usual Kondo behavior with $J \sim -V^2/E_0$. In fact, the Kondo limit corresponds to taking the limits $V \rightarrow \infty$ and $E_0 \rightarrow -\infty$ (as well as $U \rightarrow \infty$) in the Anderson model. That is why the correction due to ω_{max} is not observed in the renormalization studies of the Kondo model [2, 7] and has been also ignored in renormalization studies of the Anderson model.[10]

For a gapped conduction band ($\gamma = \infty$) with a $2D_1$ gap, it is straightforward to conclude that the exchange coupling becomes $J \sim V^2/(D_1 - E_0)$. In the case of a gapless conduction band, one also has to take into account the depletion of states near the Fermi level and a correction in the previous expression should appear. In fact, a continuous evolution between the two cases should occur as γ is varied. The real part of the self-energy, Eq. (12), and in particular its maximum, reflect this evolution. Consequently, in the gapless case one has $J \sim V^2/(\omega_{max} - E_0)$ and J_c^{-1} is given by Eq. (17) which shows two different scenarios for the gapless energy region in what concerns the Kondo resonance. For a pure power-law density of states with $\gamma \gtrsim 1$, the equivalent critical coupling will be $J_c \sim 1/\alpha D_1^\gamma = 1/\rho_0$ and therefore is reduced in comparison with the renormalization group result [2] in the spin-1/2 Kondo model by a factor γ . For $D \gg D_1$, the gapless energy region provides a cutoff to the log-like behavior of the real part of the self-energy for $\gamma = \infty$ and

$$J_c^{-1} \sim \alpha D_1^\gamma \ln(2\gamma D/D_1) = \rho_0 \ln(2\gamma D/D_1) \quad (18)$$

and therefore an important logarithmic factor is present. Note that according to Eq. (18) as γ becomes larger, the critical coupling goes to zero, contrary to the renormalization group result, $J_c \approx \gamma/\rho_0$. We suggest that this discrepancy is due to the unrealistic behavior of the density of states used in the renormalization group approach, see the discussion above. The behavior described by Eq. (18) reflects the existence of a Kondo-like peak in the impurity spectral function in the strong depletion limit, $\gamma \gg 1$ (see Fig. 6). This phenomenon can be related to the Shiba intragap states that occur near the band edges in s-wave superconductors.[13]

In Fig. 5, the spectral function for $U = \infty$ is displayed for several values of V and for temperatures above and below the Kondo temperature. These results were ob-

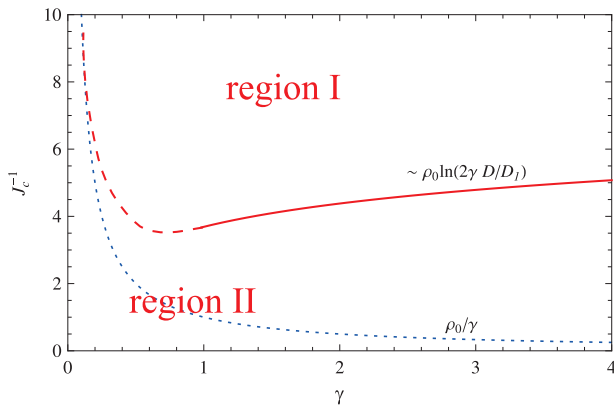


FIG. 7: Phase diagram of the gapless Anderson model in the $\gamma - J_c^{-1}$ plane. The results presented in this paper are described by the solid red line. Above the solid red line (region I), i.e., in the region with a sufficiently small exchange coupling (or equivalently, a small hybridization parameter V), the Kondo-like peak is not formed. Strong electron-electron correlations lead to a strong peak in the impurity spectral function in region II, i.e., the region of a strong exchange coupling ($J > J_c$) and a strong hybridization ($V > V_c$). The blue dotted curve represents the renormalization group result of Withoff and Fradkin [2].

tained numerically from Eq. (9) taking into account all self-energy terms. Curve a) displays the typical behavior of the impurity spectral function when $(\omega_{max} - E_0)/V^2$ is above the critical value and no Kondo resonance is observed (even at zero temperature). In curve b) of Fig. 5, a Kondo peak is present since $(\omega_{max} - E_0)/V^2$ is below the critical value. Note that this Kondo peak does not occur at $\omega = 0$ reflecting the fact that the maximum of the real part of the self-energy Σ_1 occurs at ω_{max} in contrast to the usual Kondo behavior. A broader and lower Lorentzian profile is also observed in curve b) in Fig. 5 reflecting a larger value of the hybridization. Increasing temperature above the Kondo temperature, the narrow Kondo peak disappears but a small broad peak may remain due to the depletion of the density of states at the Fermi level as explained in the discussion of the $U = 0$ case. This is the situation displayed in curve c) of Fig. 5.

For large γ , the Kondo peak emerges within the depletion region near its negative edge as shown in Fig. 6. Lowering the impurity energy level leads to the disappearance of the Kondo peak in agreement with the condition given by Eq. (17). Note that the Lorentzian profiles have similar heights and widths in Fig. 6 since the

hybridization energy is the same for all curves.

The critical coupling relation [Eq. (18)] leads to the qualitative phase diagram of Fig. 7. The renormalization group result is also displayed in this figure. A considerably larger region (region II) of resonant Kondo-like correlations induced by the strong on-site Coulomb repulsion is present in comparison with the renormalization group result (dotted blue curve in Fig. 7). This deviation becomes larger as γ grows. Note that, in this paper, we have not addressed the $\gamma < 1$ case. However, it is reasonable that as γ goes to zero, the constant density of states behavior is recovered. Our belief is that the renormalization group approach describes correctly the $\gamma \rightarrow 0$ limit and therefore, $J_c^{-1} \propto 1/\gamma$ for $\gamma \ll 1$. The dashed part of the red curve in Fig. 7 reflects this assumption.

VI. CONCLUSION

In conclusion, we have determined the critical hybridization for the Kondo effect in the gapless Anderson model. Previous works have used renormalization group approaches to the Kondo effect in gapless systems and considered a purely power-law density of states. Here we have shown that if one considers a more realistic density of states, the critical coupling expression is reduced by a logarithmic factor that reflects the fact that the Kondo effect is dominated by the contributions of the density of states away from the gapless energy region. We showed that in a gapless system, strong electron-electron correlations between conduction and impurity electrons result in a sharp Kondo-like peak if the hybridization is larger than a critical value. The critical hybridization depends on the behavior of the density of states in the depletion region and on the energy of the impurity level. The low energy critical exchange coupling J_c for the emergence of the Kondo resonance reflects the depletion of states at the Fermi energy and therefore is determined by the contribution of the states near the gapless region edge. We have demonstrated that in gapless systems, due to the strong on-site Coulomb repulsion, a sharp Kondo peak emerges much below the Fermi energy if the density of states is strongly depleted. This Kondo peak has a strong dependence on temperature. Although the results presented above rely in a specific form of the density of states, we believe that any system with a well behaved density of states (except for its gapless behavior at the Fermi energy) should display similar behavior.

-
- [1] A. H. C. Neto, F. Guinea, N. M. R. Peres, K. S. Novoselov, and A. K. Geim, *Rev. Mod. Phys.* **81**, 109 (2009).
 - [2] D. Withoff and E. Fradkin, *Phys. Rev. Lett.* **64**, 1835 (1990).
 - [3] K. Ingersent, *Phys. Rev. B* **54**, 11936 (1996).

- [4] A. Polkovnikov, S. Sachdev, and M. Vojta, *Phys. Rev. Lett.* **86**, 296 (2001).
- [5] M. Vojta and R. Bulla, *Phys. Rev. B* **65**, 014511 (2002).
- [6] J. X. Zhu and C. S. Ting, *Phys. Rev. B* **63**, 020506 (2001).
- [7] K. Sengupta and G. Baskaran, *Phys. Rev. B* **77**, 045417 (2008).

- [8] R. Bulla, T. Pruschke, and A. C. Hewson, J. Phys.: Condens. Matter **9**, 10463 (1997).
- [9] L. Fritz, M. Kircan, and M. Vojta, Physica B **359**, 77 (2005).
- [10] C. Gonzalez-Buxton and K. Ingersent, Phys. Rev. B **57**, 14254 (1998).
- [11] C. Gonzalez-Buxton and K. Ingersent, Phys. Rev. B **54**, 15614 (1996).
- [12] A. Polkovnikov, Phys. Rev. B **65**, 064503 (2002).
- [13] A. V. Balatsky, I. Vekhter, and J. X. Zhu, Rev. Mod. Phys. **78**, 373 (2006).
- [14] C. Lacroix, J. Phys. F: Metal Phys. **11**, 2389 (1981).
- [15] A. Hewson, *The Kondo Problem to Heavy fermions* (Cambridge, Cambridge Univ. Press, 1993).
- [16] D. Zubarev, Soviet Phys. Uspekhi **3**, 320 (1960).
- [17] J. A. Appelbaum and D. R. Penn, Phys. Rev. **188**, 874 (1969).